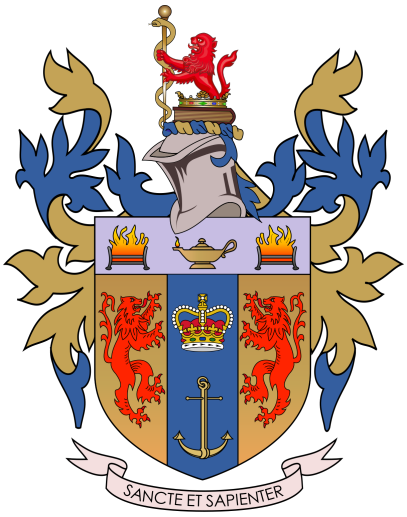

The Impact of Warm Dark Matter on Structure Formation

Dhruv Gandotra
1708050

Fourth Year Project in Physics

Submitted to King's College London
Supervisors: James Alvey, Nashwan Sabti
and Professor Malcolm Fairbairn

Department of Maths
Department of Physics

12th April 2021

Abstract

The main idea of this report was to study how warm dark matter, compared to cold dark matter, would affect structure formation. In order to do so, we started with a homogeneous and isotropic universe. We then introduced small density perturbations in our system and analysed their evolution using cosmological perturbation theory. To study the effect these fluctuations would have, we generated simulations of a cosmological observable called the matter power spectrum using a code called `CLASS`. These plots helped us understand how structure formation would be affected in the presence of cold and warm dark matter. What we found was that if there was only warm dark matter in the universe, structure formation would be significantly reduced. This finding might help explain one of the problems related to the ΛCDM model. This model predicts that there should be many more dwarf galaxies in the early stages in the universe than we can account for. This is the reason why some astrophysics theorise the existence of hot dark matter, but that comes with its own problems. That is why, warm dark matter might be the answer to both sides of this issue, acting as a middle ground to solve the dilemma of the role of dark matter in structure formation.

Contents

1 Introduction

There is a lot we do not know about the universe. Specifically, we do not know what makes up about 95% of the universe. In the standard ΛCDM model of cosmology, the total energy content of the universe contains 5% baryonic matter, 27% dark matter, and 68% dark energy. This report will focus on the dark matter section of all the energy content. Dark matter is called dark because it does not seem to interact with the electromagnetic force. Maybe it does, but very, very weakly. In other words, it does not absorb, reflect, or emit light. Therefore, it is incredibly difficult to detect [1]. Due to this mystery, we do not even know what it is made up of. However, we what we do know is that it interacts with gravity because of the influence it has on structure formation.

In the very early stages of the universe, the Friedmann solutions to general relativity describe a homogeneous universe. Shortly after, small anisotropies gradually grew and condensed the homogeneous universe into halos, galaxies, and then stars. This process is referred to as structure formation. However, if there was only ordinary matter in the universe at the time, it would be affected by radiation, the dominant element of the universe at very early times. Therefore, its density perturbations would be washed out and be unable to condense into structure. As a result, there would not have been enough time for density perturbations to grow into the galaxies and clusters currently seen. The solution to this problem is dark matter because, as we said earlier, it does not interact with radiation. Therefore, its density perturbations can grow first, resulting in potential wells for ordinary matter to collapse later, speeding up structure formation. [2]

Now, you might be thinking, how do we know if dark matter even exists? The answer lies in observational evidence. There is a lot of evidence that points to some sort of non-baryonic matter making up about 85% of all the matter content in the Universe. These include galactic rotation curves [3], velocity dispersions of stars in galaxies [4], X-rays emitted by hot gas in galaxy clusters [5], gravitational lensing [6], the cosmic microwave background (CMB) [7], the bullet cluster [8], Type Ia supernova distance measurements [7], and baryon acoustic oscillations (BAO) [9]. Another key piece of evidence is structure formation, which is the main idea of this report.

As you can see, there is overwhelming evidence in favour of dark matter. However, some astrophysicists still disagree on its existence, and reasonably so. Decades of careful and expensive research has gone into detecting dark matter, and have produced nothing yet. Also, there are some cosmological observations that are not well-explained by the model of dark matter, such as tiny discrepancies in the orbital speeds of distant stars [10][11]. Alternatives to dark matter include modified Newtonian dynamics (MOND) [12], and tensor–vector–scalar gravity (TeVeS) [13], among others. Some of these appear to fit these observations even better than dark matter. However, on the flip side, these modifications of the standard laws of general relativity do not solve the previous problems that dark matter can solve. In essence, theories like MOND are successful on the scale of galaxies, but in the enormous accumulations of cosmic bodies, dark matter is able to give us the most accurate predictions regarding their motion and distribution. Therefore, some scientists have reason to believe that the answer might be a middle ground between both these theories. Maybe, dark matter particles that can disguise themselves as modified gravity [14]. The jury is still out on the topic of dark matter, but we are not far off from learning what makes up this mysterious 27% of the entire universe.

There are many different models for dark matter particles that are being tested currently. Some of them include axions [15], sterile neutrinos [16], weakly interacting massive particles (WIMPs) [17], and primordial black holes [18]. In general, dark matter can be classified into three different categories: cold dark matter (CDM), warm dark matter (WDM), and hot dark matter (HDM). You might think that these categories are defined by the temperature of the particle, but they are actually defined by its velocity. Or, more accurately, its free streaming length (FSL) [19]. The FSL is an important quantity that describes the average distance a particle travels, before it slows down due to cosmic expansion. Primordial density fluctuations smaller than this length would be washed out by the particle's motion from over-dense to under-dense areas of space. However, larger fluctuations, at later times in the universe, would be unaffected by this phenomenon. As the names suggest, CDM has a smaller FLS than WDM, which in turn, has a smaller FSL than HDM. The FSL of dark matter particles has major implications for structure formation. A higher FSL would reduce the number of potential wells created by density fluctuations, and in turn, would reduce the amount of ordinary matter collapsing. As a result, structure formation would be reduced.

Our currently accepted cosmological model is the ΛCDM model. However, one of the biggest holes in this model that it predicts that there should be many more small, dwarf galaxies in the early universe than we can account for. This is where HDM comes in. The high FSL of HDM can help us explain this mismatch. Basically, CDM leads to a bottom-up formation of structure where galaxies form first, and then merge into galaxy clusters, while HDM would result in a top-down formation where large structures the size of galaxy clusters form first, and then fragment into galaxies [20]. However, then comes another problem. Data from the CMB is highly uniform, which suggests that ultra-relativistic particles, such as HDM, cannot form clumps as small as galaxies. This highlights a discrepancy in what HDM theory and the actual data is saying. For this very reason, WDM is theorised. WDM acts as a middle ground between CDM and HDM, causing structure formation to occur bottom-up from above their FSL, and top-down below their FSL, resulting in its FSL being roughly the same as objects big as galaxies [21]. How structure formation is affected due to the presence of WDM is what we will be discussing and analysing in this report, with the use of perturbation theory and simulations of the matter power spectrum.

This report is organised as follows. In Section 2, we will talk about some basic cosmology and general relativity concepts. Section 3 is dedicated to cosmological perturbation theory. In Section 4, we discuss the derivation and simulations of the matter power spectrum. Finally, in Section 5, we will summarise everything we have talked about and what we have learned from our results.

2 Background Cosmology

Before we get into the core of this report, we need to lay some groundwork. Firstly, we will state the cosmological principle. Then, we will lightly touch upon some basic general relativity concepts because these will help us understand the rest of the topics. Lastly, we will look at The Friedmann Equations, and the cosmic inventory. These equations dictate the evolution of the different components of the cosmic inventory, and of the universe itself.

2.1 Cosmic Geometry and Kinematics

2.1.1 The Cosmological Principle

The **cosmological principle** is a very important notion that is widely used in the field of cosmology. It is an assumption that states that the universe, on the largest scales, is homogeneous and isotropic. Homogeneity implies that the universe looks the same at every point in space, and isotropy implies the universe looks the same in every direction. We have to specify this at the largest scales ($\sim$ billions of light years) because the universe is not at all uniform at smaller scales [22]. Without this assumption, understanding the universe as a whole would be a lot more complicated that it already is.

2.1.2 Distance and Scale Factor

In an expanding universe, the distance between two stationary objects will vary with time. We call the distance which varies with expansion, proper distance, and the distance which remains constant, the co-moving distance. We will denote the reference time, t_0, with the subscript 0, usually taken to be today's value. The proper distance between two objects is given by

$$d(t) = a(t)d_0 \tag{1}$$

where $a(t)$ is the **scale factor**. By convention, we set $a(t_0) = 1$ as the value of the scale factor today.

The **Hubble parameter** is defined as

$$H(t) \equiv \frac{\dot{a}(t)}{a(t)} \tag{2}$$

where $\dot{a}(t) \equiv da/dt$. Substituting a(t) also gives us **Hubble's law**: $\dot{d}(t) = H(t)d(t)$. The **Hubble constant** is defined as H_0. It corresponds to the value of the Hubble parameter at the time of observation. Its exact value is still a topic of experimental debate because different ways of calculating it give different measurements, but it is understood to be approximately 67-74 km/s/Mpc [23].

2.1.3 Spacetime and Metric

The cosmological principle can only be satisfied by three types of spaces. Flat space (plane), hyperbolic space (negative curvature), and spherical space (positive curvature). Surprisingly, experimental data has shown that our universe is almost completely flat.

The simplest metric with spacetime curvature which is homogeneous across space, but can vary in time, is the **Friedmann-Lemaitre-Robertson-Walker (FLRW) metric**:

$$ds^2 = -dt^2 + a(t)^2 \left[\frac{dr^2}{1 - kr^2} + r^2 \, d\Omega^2 \right] \tag{3}$$

where $k = +1/0/-1$ (curvature), and $d\Omega^2 \equiv d\theta^2 + \sin^2\theta \, d\phi^2$, which is the solid angle term. As previously mentioned, we assume that the universe is practically flat, which means we take $k = 0$ [24].

2.2 Cosmic Dynamics

2.2.1 The Friedmann Equations

Now, we will do a simplified derivation of the Friedmann equations. Firstly, we differentiate the FLRW metric to get the Christoffel symbols. Next, using these and their derivatives, we can get the **Ricci tensor**, $R_{\mu\nu}$, and the **Einstein tensor**, $G_{\mu\nu}$. These tensors are then related by the **Einstein equation**.

$$R_{\mu\nu} - \frac{1}{2} R g_{\mu\nu} \equiv G_{\mu\nu} = 8\pi G T_{\mu\nu} \tag{4}$$

where $T_{\mu\nu}$ is the **stress-energy tensor**.

We can then apply the cosmological principle to the stress-energy tensor, i.e. the net momentum and vorticity of the universe must be zero to maintain homogeneity and isotropy. Therefore,

$$\begin{aligned} T_{00} &= -\rho \\ T_{0i} &= 0 \\ T_{ij} &= \delta_{ij} P \end{aligned} \tag{5}$$

where ρ is the energy density and P is the pressure. We will soon see how they are linked.

The solutions for $R_{\mu\nu}$ and $T_{\mu\nu}$ give us two solutions to the Einstein tensor:

$$\begin{aligned} G^0_0 &= -3H^2 - 3\frac{k}{a^2} = -8\pi G\rho \\ G^i_j &= -(H^2 + 2\frac{\ddot{a}}{a} + \frac{k}{a^2}) \\ \delta_{ij} &= -8\pi G P \end{aligned} \tag{6}$$

and the remaining components of $G_{\mu\nu}$ are all equal to zero.

By manipulating these two equations, we get

$$H^2 = \frac{8\pi G}{3}\rho - \frac{k}{a^2} \tag{7a}$$

$$\frac{\ddot{a}}{a} = -\frac{4\pi}{3} G(\rho + 3p) \tag{7b}$$

$$\dot{\rho} = -3H(\rho + p) \tag{7c}$$

Equation 7a is called the **Friedmann equation**; Equation 7b is called the **acceleration equation**, and Equation 7c is called the **conservation cquation**. Collectively, they are called the **Friedmann equations** [24][25].

2.2.2 The Cosmic Inventory

The universe is full of different kinds of stuff, so in general, $\rho_{\text{total}} = \rho_x + \rho_y + \rho_z + \ldots$, where x, y, z can be anything from matter to radiation to dark energy. Solving the Friedmann equation for $k = 0$ gives us the **critical density**, the density which defines a flat universe.

$$\rho_{\text{crit}} \equiv \frac{3H^2}{8\pi G} \tag{8}$$

From this, we can define the **density parameter** of any given type of energy density, χ,

$$\Omega_\chi \equiv \frac{\rho_\chi}{\rho_{\text{crit}}} \tag{9}$$

The density parameter for all the different types of energy in the universe, Ω_{tot}, corresponds to the curvature of the universe: $\Omega_{tot} > 1$ (k = 1) is a closed universe; $\Omega_{tot} < 1$ (k = –1) is an open one; and $\Omega_{tot} = 1$ (k = 0) is a flat universe. Now, we will discuss the different energy components of the universe, and how they evolve over time.

- **Matter**
  This refers to all forms of matter for which the pressure is much smaller than the energy density, $|P| \ll \rho$. This happens when the energy density is dominated by the mass a gas of non-relativistic particles.
  - Baryons: Ordinary matter such as nuclei and electrons
  - Dark Matter: Most of the matter in the universe is in the form of invisible dark matter.
- **Radiation**
  This refers to anything for which the pressure is about a third of the energy density, $P = \rho/3$. This happens when the energy density is dominated by the kinetic energy, i.e. the momentum is much bigger than the mass. For example, a gas of relativistic particles.
  - Photons: Massless, chargeless, always relativistic particles
  - Neutrinos: Similar to an electron, but have no electrical charge and very small masses. There are three flavours of neutrinos, and they are one of the most abundant particles in the universe.
  - Gravitons: Hypothetical elementary particle that carry the force of gravity. Today, many experiments are trying to detect them.
- **Dark Energy**
  Recently, scientists have realised that there needs to be another mysterious component in the universe which is driving the universe's accelerated expansion. This component seems to have a negative pressure, $P = -\rho$. We know even less about dark energy than dark matter.

Summary

We can parameterise most cosmological fluids using an **equation of state**, $\omega = P/\rho$. This means that $\omega = 0$ for matter, $\omega = 1/3$ for radiation, and $\omega = -1$ for dark energy. Then, using the conservation equation (Equation 7c), we can get a relation between the energy density and the scale factor.

$$\rho \propto a^{-3(1+\omega)} \tag{10}$$

Using this relation,

$$\rho \propto \begin{cases} a^{-3} & \text{for matter} \\ a^{-4} & \text{for radiation} \\ a^{0} & \text{for dark energy} \end{cases} \tag{11}$$

For a spatially flat universe ($k = 0$), the solution for the scale factor is

$$a(t) \propto t^{\frac{2}{3(w+1)}} \tag{12}$$

Therefore,

$$a(t) \propto \begin{cases} t^{2/3} & \text{for matter} \\ t^{1/2} & \text{for radiation} \\ e^{(t\sqrt{\Lambda/3})} & \text{for dark energy} \end{cases} \tag{13}$$

where Λ is the cosmological constant and is approximately 2 x 10^{-35} s^{-2} [23][24].

3 Cosmological Perturbation Theory

Until now, we treated the universe as homogeneous. However, to understand the formation and evolution of large-scale structures, we need to introduce fluctuations. As long as these perturbations remain relatively small, we can treat them in perturbation theory. For simplicity, we will only consider a matter-dominated universe. Also, we are only going to be looking at Newtonian perturbation theory, because GR perturbation theory can be very complicated. In addition, at small scales and low velocities, Newtonian perturbation theory is enough to give us a general picture of what is happening.

In order to do so, we need to look at the three fluid equations: Continuity, Euler and Poisson. These equations and their solutions will help us understand how energy evolves in different settings of space due to the effect of density fluctuations. To make things easier, we will perform a transformation of variables and only work in the linear regime. Finally, we will briefly discuss the concept of Fourier transforms, and why they are useful for us.

3.1 The Fluid Equations

The primary sources of structure formation are perturbations in energy density and number density. These fluctuations cause some areas in space to have deeper or shallower gravitational wells, which in turn draws more or less matter. These perturbations then

evolve and grow over time into the galaxies and clusters of galaxies we see today. However, to properly analyse these effects, we first need to start with the unperturbed equations of motion.

3.1.1 Continuity Equation

The first fluid equation is the **continuity equation**, or energy equation, and it comes from energy (mass) conservation. It guarantees that the change of mass in a particular volume of space is equal to the net amount of matter flowing into the volume, or flux. Considering a matter-dominated universe, the Newtonian continuity equation is

$$\left(\frac{\partial \rho}{\partial t}\right)_{\mathbf{r}} + \nabla_{\mathbf{r}} \cdot (\rho \mathbf{u}) = 0 \tag{14}$$

where $\rho(\mathbf{r}, t)$ is the mass density, and $\mathbf{u}(\mathbf{r}, t)$ is the velocity [26][27].

3.1.2 Euler Equation

The second fluid equations is the **Euler equation**, or force equation, and it comes from momentum conversation. This equation considers the sources of velocity flows in the fluid. In particular, the two forces we take into account are the gravitational force, the total gravitational attraction by all matter in the universe, and the force due to pressure in the fluid.

$$\left(\frac{\partial \mathbf{u}}{\partial t}\right)_{\mathbf{r}} + (\mathbf{u} \cdot \nabla_{\mathbf{r}})\, \mathbf{u} = -\nabla_{\mathbf{r}} \Phi \tag{15}$$

where Φ is the gravitational potential. In essence, this is Newton's Second Law for a fluid, with the acceleration of the fluid on the left side, and the accelerating gravitational force terms on the right [26][27].

3.1.3 Poisson Equation

Now that we know that the sources of velocity in the fluid are the gravitational potential and the pressure, we need to establish what their ultimate source is. The gravitational potential is caused by the total cosmic matter and the energy density. Even though this involves contributions by radiation and dark energy components, in a matter-dominated universe, we can ignore them and only take the matter density as a source of the gravitational potential. Therefore, the Newtonian form of the **Poisson equation** is

$$\nabla_{\mathbf{r}}^2 \Phi = 4\pi G \rho \tag{16}$$

where G is the gravitational constant [26][27].

Summary

These three equations are collectively known as the **fluid equations**. For a matter-dominated universe, the Newtonian form of these equations are

$$\text{Continuity}: \left(\frac{\partial \rho}{\partial t}\right)_{\mathbf{r}} + \nabla_{\mathbf{r}} \cdot (\rho \mathbf{u}) = 0 \tag{17a}$$

$$\text{Euler}: \left(\frac{\partial \mathbf{u}}{\partial t}\right)_{\mathbf{r}} + (\mathbf{u} \cdot \nabla_{\mathbf{r}})\, \mathbf{u} = -\nabla_{\mathbf{r}} \Phi \tag{17b}$$

$$\text{Poisson}: \nabla_{\mathbf{r}}^2 \Phi = 4\pi G \rho \tag{17c}$$

3.2 Perturbations

Now, we will introduce perturbations to our system because we want to analyse the evolution of these perturbations with respect to the background FRLW universe. However, we need to make a couple adjustments before we do so.

3.2.1 Change in Coordinates

Until now, we have been using physical coordinates, $\mathbf{r}$. However, it is easier to introduce perturbations in comoving coordinates, $\mathbf{x}$. After transforming coordinates (Appendix A), we will use the density perturbation, $\delta(\mathbf{x}, t)$ instead of the density, $\rho(\mathbf{r}, t)$, as defined by

$$\rho(\mathbf{r}) = \bar{\rho}(1 + \delta(\mathbf{x}, t)) \tag{18}$$

where $\bar{\rho}$ is the background density. We will assume that this density field, $\delta(\mathbf{x}, t)$, is a **Gaussian random field**, and that it obeys Gaussian statistics (Appendix B). We will later see why this is useful. Also, instead of the gravitational potential, $\mathbf{\Phi}$, we will use the potential perturbation, ϕ, where

$$\phi \equiv \Phi - \frac{2}{3}\pi G\bar{\rho}a^2x^2 \tag{19}$$

By making the appropriate substitutions, we can now write a *coordinate transformed* version of the fluid equations. From now on, we will also drop the subscript $\mathbf{x}$.

$$\text{Continuity}: \frac{\partial\delta}{\partial t} + \frac{1}{a}\vec{\nabla}\cdot((1+\delta)\mathbf{v}) = 0 \tag{20a}$$

$$\text{Euler}: \frac{\partial\mathbf{v}}{\partial t} + \frac{1}{a}(\mathbf{v}\cdot\nabla)\,\mathbf{v} + \frac{\dot{a}}{a}\mathbf{v} = -\frac{1}{a}\nabla\phi \tag{20b}$$

$$\text{Poisson}: \nabla^2\phi = 4\pi G\bar{\rho}a^2\delta \tag{20c}$$

In essence, we have transformed the fluid equations with respect to physical coordinates and in terms of physical quantities, to a set of fluid equations with respect to comoving coordinates and in terms of perturbation quantities [24][26][27].

3.2.2 Linear Evolution

If you look at the fluid equations in Equation 20, there are some non-linear terms such as $\delta(\mathbf{x})\mathbf{v}$ in the continuity equation, and $(\mathbf{v}\cdot\vec{\nabla}_x)\mathbf{v}$ in the Euler equation, which make the system insolvable for generic density and velocity fields, and thus, very difficult to analyse. Therefore, we need to make an assumption that the density and velocity perturbations are still very small.

This assumption is justified by the fact that on all scales, primordial fluctuations were extremely small, $\delta \ll 1$. In other words, the first instances of structure formation were linear in character. We will discuss more in the next section. Due to this linear regime, we can discard these negligible higher order terms, resulting in a fully solvable set of *linearised* set of fluid equations [27].

$$\text{Continuity}: \frac{\partial \delta}{\partial t} + \frac{1}{a}\vec{\nabla} \cdot \mathbf{v} = 0 \tag{21a}$$

$$\text{Euler}: \frac{\partial \mathbf{v}}{\partial t} + \frac{\dot{a}}{a}\mathbf{v} = -\frac{1}{a}\vec{\nabla}\phi \tag{21b}$$

$$\text{Poisson}: \nabla^2\phi = 4\pi G\bar{\rho}a^2\delta \tag{21c}$$

Solutions

From Equation 21, we can derive the time evolution of the density perturbation $\delta(\mathbf{x}, t)$. The first step is to take the divergence of the Euler equation.

$$\frac{\partial}{\partial t}(\nabla \cdot \mathbf{v}) + \frac{\dot{a}}{a}(\nabla \cdot \mathbf{v}) = -\frac{1}{a}\nabla^2\phi \tag{22}$$

The next step is to manipulate the continuity equation (21a), as follows.

$$\nabla \cdot \mathbf{v} = -a\frac{\partial \delta}{\partial t} \tag{23}$$

Now, we can substitute Equation 23 and the Poisson equation into Equation 22 to get a second order PDE for $\delta(\mathbf{x}, t)$.

$$\frac{\partial^2 \delta}{\partial t^2} + 2\frac{\dot{a}}{a}\frac{\partial \delta}{\partial t} = 4\pi G\bar{\rho}\delta \tag{24}$$

This is the linearised equation for the growth of density perturbations, $\delta(\mathbf{x}, t)$. The fact that is a second order PDE implies two things for us. Firstly, one can see that it has two solutions.

$$\delta(\mathbf{x}, t) = \delta_1(\mathbf{x}, t) + \delta_2(\mathbf{x}, t) \tag{25}$$

Secondly, the fact that it only has derivatives in time implies that the time evolution is independent of the location, $\mathbf{x}$. This means that the corresponding solution can be split into a spatial part, $\Delta(\mathbf{x})$, and a temporal part, $D(t)$, such that, $\delta(t) = D(t)\Delta(\mathbf{x})$, where the time evolution, $D(t)$, is

$$\frac{\partial^2 D}{\partial t^2} + 2\frac{\dot{a}}{a}\frac{\partial D}{\partial t} = 4\pi G\bar{\rho}D \tag{26}$$

Both these results can be combined to give us a general linear solution.

$$\begin{aligned} &\delta_1(\mathbf{x}, t) = D_1(t)\,\Delta_1(\mathbf{x}) \\ &\qquad\qquad \Longrightarrow \delta(\mathbf{x}, t) = D_1(t)\,\Delta_1(\mathbf{x}) + D_2(t)\,\Delta_2(\mathbf{x}) \\ &\delta_2(\mathbf{x}, t) = D_2(t)\,\Delta_2(\mathbf{x}) \end{aligned} \tag{27}$$

where $D_1(t)$ and $D_2(t)$ are the **density growth factors** for the linear evolution of the density perturbations, and $\Delta_1(\mathbf{x})$ and $\Delta_2(\mathbf{x})$ represent the corresponding spatial configuration of the cosmic primordial matter distribution. From this result, we can directly observe that the rate at which the primordial densities grow in the linear regime is the same everywhere, and solely depend on the global time factors, $D_1(t)$ and $D_2(t)$. [26][27]

3.2.3 Fourier Transforms

A more convenient way of solving the PDEs in Equation 21 is via Fourier analysis. This process involves transforming equations by expanding them into their Fourier components. Essentially, **Fourier transforms** decompose functions depending on space or time into functions depending on spatial or temporal frequency. In our case, it turns PDEs into ODEs, which are easier to solve. Now, we will try and derive our fluid equations in Fourier space. The first step is to Fourier transform the three fields that we have (Appendix C).

$$\text{Density Field}: \delta(\mathbf{x}) = \int \frac{d^3\mathbf{k}}{(2\pi)^3}\,\hat{\delta}(\mathbf{k})\,e^{-i\mathbf{k}\cdot\mathbf{x}} \iff \hat{\delta}(\mathbf{k}) = \int d^3\mathbf{x}\,\delta(\mathbf{x})\,e^{i\mathbf{k}\cdot\mathbf{x}} \tag{28a}$$

$$\text{Velocity Field}: \mathbf{v}(\mathbf{x}) = \int \frac{d^3\mathbf{k}}{(2\pi)^3}\,\hat{\mathbf{v}}(\mathbf{k})\,e^{-i\mathbf{k}\cdot\mathbf{x}} \iff \hat{\mathbf{v}}(\mathbf{k}) = \int d^3\mathbf{x}\,\mathbf{v}(\mathbf{x})\,e^{i\mathbf{k}\cdot\mathbf{x}} \tag{28b}$$

$$\text{Potential Field}: \phi(\mathbf{x}) = \int \frac{d^3\mathbf{k}}{(2\pi)^3}\,\hat{\phi}(\mathbf{k})\,e^{-i\mathbf{k}\cdot\mathbf{x}} \iff \hat{\phi}(\mathbf{k}) = \int d^3\mathbf{x}\,\phi(\mathbf{x})\,e^{i\mathbf{k}\cdot\mathbf{x}} \tag{28c}$$

where $\mathbf{k}$ is a spatial parameter called a **Fourier mode**. Small values of $\mathbf{k}$ signify large scales, and large values of $\mathbf{k}$ signify small scales. A Fourier mode, more specifically, is a wave that oscillates sinusoidally in space. We can add up our Fourier modes, via integration, to give us back our $f(\mathbf{x})$.

Finally, by substituting Equation 21 with the Fourier versions of the fields, in Equation 28, and their spatial derivatives (Appendix C), we can get the *Fourier transformed* set of the fluid equations.

$$\begin{aligned}
\text{Continuity}: \frac{d\hat{\delta}(\mathbf{k})}{dt} - \frac{1}{a} i\mathbf{k}\cdot\hat{\mathbf{v}}(\mathbf{k}) = 0 \\
\text{Euler}: \frac{d\hat{\mathbf{v}}(\mathbf{k})}{dt} + \frac{\dot{a}}{a}\mathbf{v}(\mathbf{k}) = \frac{1}{a} i\mathbf{k}\cdot\hat{\phi}(\mathbf{k}) \\
\text{Poisson}: \frac{\hat{\phi}(\mathbf{k})}{a^2} = -4\pi G\,\bar{\rho}\,\frac{\hat{\delta}(\mathbf{k})}{k^2}
\end{aligned} \tag{29}$$

From this set of equations, the main observation is that in the linear regime, each Fourier mode, $\mathbf{k}$, evolves independently of all other modes. Also, we will only consider large scales because on small scales and at low redshift, gravitational collapse is non-linear, which can then be computed accurately using N-body simulations. Therefore, higher-order statistics are necessary to describe the full field at small scales. However, on large scales, structures grow according to linear theory. Thus, in this regime, the density field can be completely described by the power spectrum, as it is a Gaussian random field [26][27].

4 The Matter Power Spectrum

Now, we will try and connect everything we have discussed so far. One of the main observables in cosmology is the power spectrum, which is a very general concept that can be used to describe many different quantities. However, we will specifically be using it for the matter content of the universe, Ω_m, which includes baryons and dark matter. Therefore, in our case, it will be referred to as the matter power spectrum (MPS).

We used a powerful Boltzmann code called `CLASS` (Cosmological Linear Anisotropy Solving System) in C++ to predict and visualise the MPS in the presence of warm dark matter (WDM) to see the effect it would have on structure formation. However, to fully understand the MPS, we still need a few key concepts.

4.1 The Mathematics

4.1.1 Correlation Function

The first step to deriving the MPS is to start with the density field, $\delta(\mathbf{x}, t)$. Now, the problem is that how can we describe this field without having to specify its actual value at each location in space-time? Therefore, we use something called **ensemble averages**. In our case, $\langle\delta(\mathbf{x})\rangle$ describes the average density at $\mathbf{x}$ for many realisations of the random process.

However, observationally, we only have access to one realization of this random process. Thanks to the **ergodic hypothesis**, which states that *the ensemble average is equal to the spatial average taken over one realization of the random field* [28], we can use this average to represent the entire random field. We can use this notion because we are using Gaussian random fields (Appendix B), for which this hypothesis is proved [27]. The next step is to Fourier transform the density field, like in Equation 28a.

$$\delta(\mathbf{x}) = \int \frac{d^3\mathbf{k}}{(2\pi)^3}\,\hat{\delta}(\mathbf{k})\,e^{-i\mathbf{k}\cdot\mathbf{x}} \tag{30}$$

Now, we define the 2-point **correlation function**, $\xi(r)$ as follows.

$$\xi(r) \equiv \langle\delta(\mathbf{x})\delta(\mathbf{x}+\mathbf{r})\rangle \tag{31}$$

where the angled brackets indicate an average over, in our case, the entire space. The correlation function is commonly described as "*Given a random galaxy in a location, the correlation function describes the probability that another galaxy will be found within a given distance*" [28].

4.1.2 Power Spectrum

Since $\delta(\mathbf{x})$ is real, $\hat{\delta}^*(\mathbf{k}) = \hat{\delta}(-\mathbf{k})$. Therefore, with some algebraic manipulation, we obtain the following.

$$\xi(r) = \left\langle\hat{\delta}(\mathbf{k})\hat{\delta}(\mathbf{k}')\right\rangle = (2\pi)^3\delta_D\left(\mathbf{k}-\mathbf{k}'\right)P(k) \tag{32}$$

where $\delta_D()$ is a Dirac delta function, and $P(k)$ is the **matter power spectrum**. The MPS describes the density contrast of the universe as a function of scale.

Thanks to our knowledge of Fourier transforms, we can see that the power spectrum and the correlation function are essentially Fourier transform pairs.

$$\xi(r) = \int \frac{d^3\mathbf{k}}{(2\pi)^3}\,P(k)\,e^{-i\mathbf{k}\cdot\mathbf{r}} \implies P(k) = \hat{\xi}(k) \tag{33}$$

Some books use a different notation for the power spectrum. Since $P(k)$ has dimensions of length^3, $k^3\,P(k)$ is dimensionless. Therefore, we can define the **dimensionless power spectrum**, as follows.

$$\Delta^2(k) \equiv \frac{k^3 P(k)}{2\pi^2} \Longrightarrow \xi(r) = \int \frac{dk}{k} \Delta^2(k) \tag{34}$$

Therefore,

$$\Delta^2(k) = \frac{d\langle\delta^2(\mathbf{x})\rangle}{d\,ln\,k} \tag{35}$$

where $\langle\delta^2(\mathbf{x})\rangle = \xi(0) = \sigma^2(\mathbf{x})$ is the zero-lag correlation function, or the variance of the density field (Appendix B). This notation is useful because it measures the contribution of perturbations per unit logarithmic interval at wave number, $\mathbf{k}$, to the variance in the matter density fluctuations. [28][29][30]

4.1.3 Transfer Function

To get the final form of the power spectrum, we need to consider the **primordial matter power spectrum**, $P_0(k)$. The primordial MPS is assumed to have a power law characterisation, such that

$$P_0(k) = A_s k^{n_s} \tag{36}$$

where k^{n_s} is the scaling factor, n_s is a free parameter, and A_s is a normalisation constant. There are multiple models for thus dependency, but the simplest one is called the Harrison-Zeldovich spectrum and it assumes that $n_s = 1$, in line with a "flat" scale-invariant spectrum.

Now we include the **transfer function**, $T(k)$. It describes the evolution of perturbation theory through epochs of horizon crossing and radiation-matter equality (RME), and basically mediates the transition from the universe being radiation dominated (very early universe) to being matter dominated (middle period). In other words, it relates the processed MPS to its primordial form, $P(k) = P_0(k)\,T^2(k)$. However, one thing to remember is that $\delta^2(\mathbf{x}, t) = D^2(t)\,\delta^2(\mathbf{x})$, where $D(t)$ is the linear growth factor in density. This growth function describes the scale-independent growth at later times in the universe. Therefore, we finally have the complete form of the MPS.

$$P(k) = P_0(k)\,T^2(k)\,D^2(t) \tag{37}$$

The MPS is proportional to δ^2. At large scales (small k), $P \propto k$, and the transfer function is unity. At small scales (large k), the MPS turns over, and the mode enters the horizon well before RME. During the radiation epoch, the potential decays (slowly), and the transfer function is much smaller than unity. Modes that enter much earlier are even more suppressed. Therefore, the MPS is a decreasing function of k on small scales [29][30].

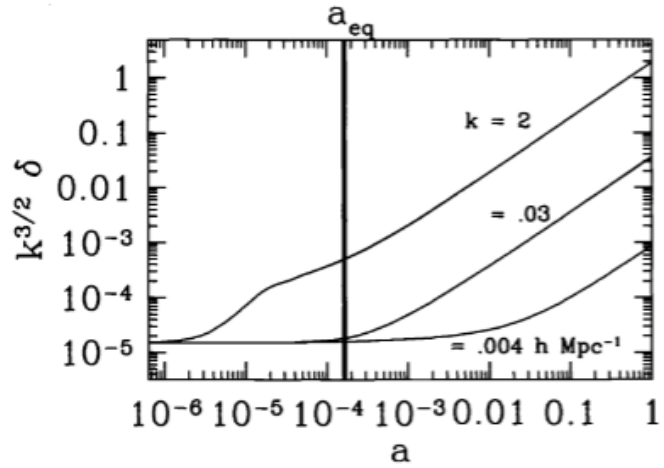

Figure 1: The evolution of perturbations to the dark matter. Amplitude starts to grow upon horizon entry (different times for the three different modes shown here). Well after a_{eq}, all sub-horizon modes evolve identically, scaling as the growth factor [29].

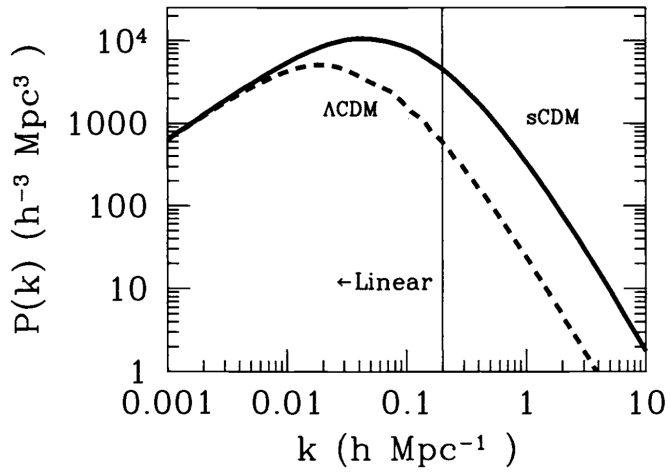

Figure 2: The MPS in two CDM models, with a cosmological constant (ΛCDM) and without one (sCDM). The spectrum in the cosmological constant model turns over on larger scales because of a later a_{eq}. Scales to the left of the vertical line are still evolving linearly [29].

4.2 The Simulations

Now, we can start visualising the MPS. The reason why we need `CLASS` is because for a CDM particle, its momentum is much lower than its energy, $p \ll E$. Therefore, we can ignore higher order momentum terms in its Maxwell-Boltzmann distribution and we can use the linear fluid equations to analyse the evolution of a CDM particle. However, for a WDM particle, that is not the case anymore. Its momentum is too high to ignore, relative to its energy, $p \sim E$. Therefore, the higher order momentum terms are not negligible anymore, and we cannot use the fluid equations to model WDM. That is why we need `CLASS` to simulate the presence of WDM in our system, by adjusting different parameters. However, to study the impact of WDM, we need to have a base CDM MPS to compare with.

4.2.1 Method

The main purpose of `CLASS` is to simulate the evolution of linear perturbations in the universe, and to compute CMB (Cosmic Microwave Background) and LSS (Large Scale Structure) observables. [31]. Firstly, we had to select reference values of cosmological parameters to produce a CDM MPS. We used the following table as our parameter values for this simulation.

Parameter	Values	Description
H_0 $\left[\text{km s}^{-1}\ \text{Mpc}^{-1}\right]$	67.27	Hubble parameter
T_{CMB}	2.7255	Photon density (in K)
$\Omega_{\text{b}}h^2$	0.02236	Baryon density
$\Omega_{\text{c}}h^2$	0.1202	CDM density
N_{nCDM}	0	Number of non-CDM species (including WDM)
τ	0.0544	Optical depth to reionisation (RME)
output	mPk,mTk	Output spectra requested
Pk_ini	analytic_Pk	Primordial spectrum type
$\ln\left(10^{10}A_{\text{s}}\right)$	3.045	Normalisation constant (Equation 36)
n_{s}	0.9649	Free parameter (Equation 36)
Pk_max_h	10	Maximum k in P(k)

Table 1: Combination of some values from Table 2 of [32] and some values in `CLASS`

This whole list of parameters, along with some extra ones, was then set in the input file, generating an output CSV file with two columns, k (h/Mpc) and $P(k)$ (Mpc/h)^3. From there, we plotted the CSV file in Python to produce our reference CDM MPS.

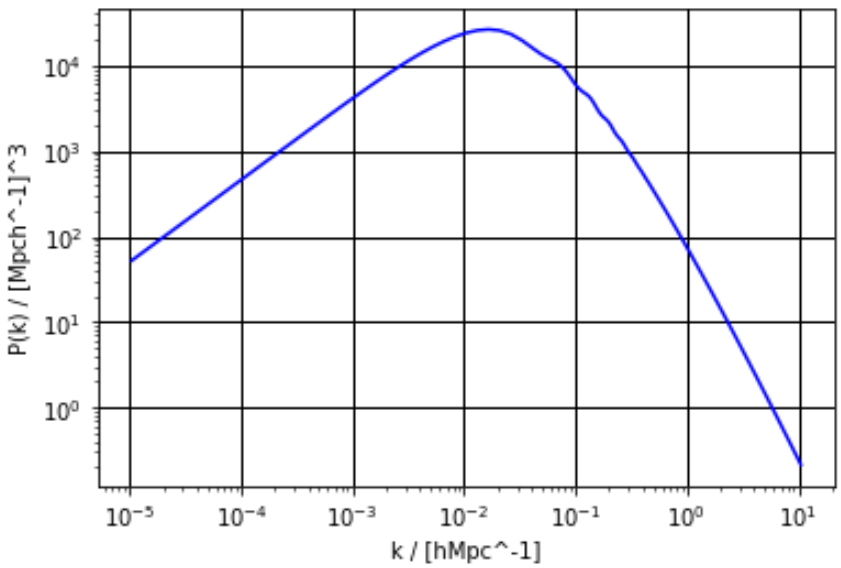

Figure 3: CDM MPS generated using parameters in Table 1

Similarly, we also generated WDM MPS plots by adjusting different parameters. We will now compare those plots with this CDM MPS to study the impact WDM would have on structure formation.

4.2.2 Results and Analysis

For the WDM MPS plots, we changed some of the cosmological parameters so that we can model the Universe as if there was WDM instead of CDM. We assumed that the WDM is a thermal relic, and that it follows a Gaussian distribution. However, the default distribution of a non-CDM species in `CLASS` is a Fermi-Dirac distribution. Therefore, we had to implement the Gaussian distribution into our code. After doing so, we gained access to two extra parameters related to the Gaussian distribution, the average momentum of the distribution (y^*) and the variance of the distribution (σ). Here is the summary of the changes that we made.

Parameter	Values	Description
$\Omega_c h^2$	0	CDM density
N_{nCDM}	1	Number of non-CDM species (WDM)
Ω_{nCDM}	0.12038	WDM density
m_{nCDM}	1-9	Mass of WDM particle (in keV)
T_{nCDM}	0.1-0.9	Temperature of WDM particle
ncdm_psd_parameters	3-20, 3-20	average momentum (y^*) and variance (σ)

Table 2: New values of the cosmological parameters used in `CLASS` for the WDM MPS simulations. The four variables with the range of values were the parameters that we adjusted in the simulations to test our hypothesis.

While testing each of the four variables, we needed to choose reference values for the other three controlled variables. We picked 1 keV, 0.71611 K, 20, 20 for the mass, temperature, average momentum, and variance respectively. The specific value of 0.71611 K is a default value in `CLASS` and is very close to the instantaneous decoupling temperature of active neutrinos, $(4/11)^{1/3}$ K. It is slightly higher to be in line with precise current research of active neutrino decoupling [33]. This time, along with the usual input file, we also needed to use a precision file called `pk_ref.pre` to increase the precision of our plots.

The first variable we tested was the mass of the WDM particle.

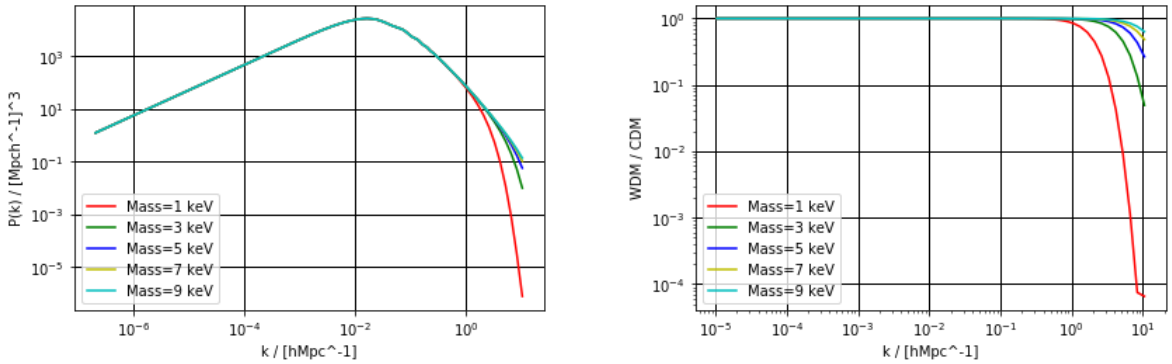

(a) WDM MPS (b) WDM/CDM

Figure 4: Simulations of the WDM MPS for different particle masses

From Figure 4, we can see that increasing the mass of our WDM particle does not have any effect on the MPS at large scales (k $<$ 1 h/Mpc). However, at smaller scales, the power spectrum is getting less suppressed. Also, the ratio WDM/CDM is approaching 1, at small scales, as we increase the mass. This makes sense, since if we have a heavier WDM particle, it would act similar to a CDM particle because it would stay relativistic for a shorter period of time. Therefore, it would have a lower FSL. This means that **increasing the mass of the WDM particle has a positive effect on structure formation**.

The second variable we tested was the temperature of the WDM particle.

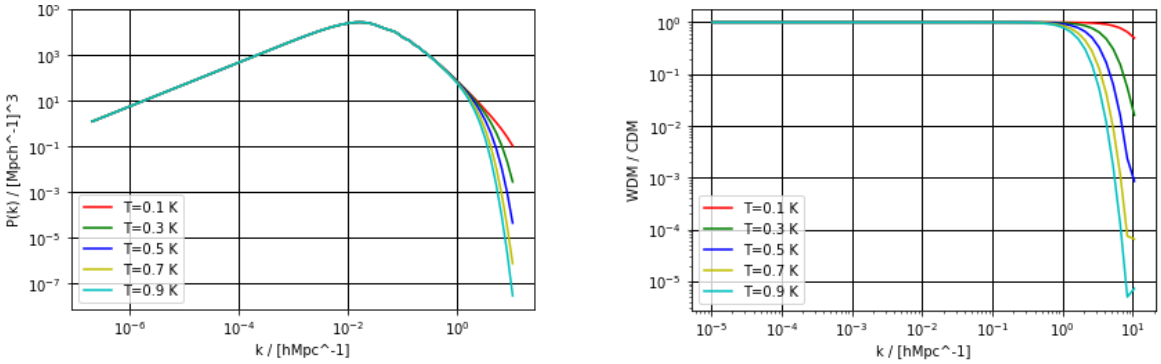

(a) WDM MPS (b) WDM/CDM

Figure 5: Simulations of the WDM MPS for different particle temperatures

Similar to the previous plots, we can see that increasing the temperature of our WDM particle does not have any effect on the MPS at large scales (k $<$ 1 h/Mpc). However, unlike the mass, at smaller scales, the power spectrum is getting more suppressed. Also, the ratio WDM/CDM is diverging from 1, at small scales, as we increase the temperature. This also makes sense, since if we have a hotter WDM particle, it would act less like a CDM particle because it would stay relativistic for a longer period of time. Therefore, it would have a higher FSL. This means that **increasing the temperature of the WDM particle has a negative effect on structure formation**.

The final two variables we tested were the average momentum (y^*) and the variance of the distribution (σ). However, we found that changing these variables had no effect on the WDM MPS. This might be due to our WDM particle mass range being too high for any of these variables to have an effect on the MPS.

5 Conclusion

The purpose of this report was to study the impact of warm dark matter on structure formation. We did this using a code called `CLASS` which simulated the presence of warm dark matter and its effect on the evolution of linear perturbations in the Universe. However, we needed some theory to fully understand the results. We started with some background cosmology concepts, including the Friedmann equations. These equations described the evolution of space in a homogeneous and isotropic universe. Next, we moved on to perturbation theory, and introduced the fluid equations. These equations helped us understand how different fields evolved over time. We then introduced linear perturbations to these fields and analysed how the fluid equations changed accordingly.

Finally, we moved onto a cosmological observable called the matter power spectrum. We talked about its derivation and what its plots mean for studying structure formation. After that, we ran simulations in `CLASS` for cold and warm dark matter, by adjusting a set of parameters. The reason why we needed `CLASS`, for warm dark matter specifically, was that we cannot model the warm dark matter as a fluid, like we did for cold dark matter. This was because in the Maxwell-Boltzmann velocity distribution of dark matter, there are some higher order momentum terms. For cold dark matter, we ignored these terms because its momentum is negligible, relative to its energy, and we can analytically study its evolution with the linear fluid equations. However, for warm dark matter, its momentum is too high, relative to its energy, to ignore the higher order momentum terms.

The results we produced correlated with what we suspected. Warm dark matter has a higher free streaming length than cold dark matter, and that would reduce the number of potential wells created by baryon clumping. Therefore, compared to cold dark matter, structure formation would be reduced in the presence of warm dark matter. Our results showed that decreasing the mass, or increasing the temperature of the WDM particle, (i.e. less "cold"), suppressed the matter power spectrum, which signifies reduced structure formation, as we predicted.

Appendices

A: Transformation of Variables

In an expanding spacetime, we have the following relation between the physical coordinates, $\mathbf{r}$, and the comoving coordinates. $\mathbf{x}$.

$$\mathbf{r}(t) = a(t)\mathbf{x} \tag{38}$$

Therefore, a velocity field, $\mathbf{u}(t) = \dot{\mathbf{r}}$, will be given by $\mathbf{u}(t) = H\mathbf{r} + \mathbf{v}$. From these two relations, we can get the **proper velocity**, $\mathbf{v} = \mathbf{u} - (\dot{a}/a)\mathbf{r} = (a\mathbf{x}) - \dot{a}\mathbf{x} = a\dot{\mathbf{x}}$.

Also, in a static spacetime, the time and space derivatives defined for the parameters $\mathbf{r}$ and t are independent. However, in an expanding spacetime, this is not the case anymore. Therefore, we need to transform both derivatives accordingly. Firstly, we need to use space derivatives defined with respect to the comoving coordinates, $\mathbf{x}$, denoted as $\nabla_{\mathbf{x}}$. From Equation 38, we can get the relation,

$$\nabla_{\mathbf{r}} = a^{-1}\nabla_{\mathbf{x}} \tag{39}$$

We can also transform the time derivatives at fixed r to the time derivatives at fixed x, as follows [24].

$$\begin{aligned}\left(\frac{\partial}{\partial t}\right)_{\mathbf{r}} &= \left(\frac{\partial}{\partial t}\right)_{\mathbf{x}} + \left(\frac{\partial \mathbf{x}}{\partial t}\right)_{\mathbf{r}} \cdot \nabla_{\mathbf{x}} \\ &= \left(\frac{\partial}{\partial t}\right)_{\mathbf{x}} + \left(\frac{\partial a^{-1}\mathbf{r}}{\partial t}\right)_{\mathbf{r}} \cdot \nabla_{\mathbf{x}} \\ &= \left(\frac{\partial}{\partial t}\right)_{\mathbf{x}} - H\mathbf{x} \cdot \nabla_{\mathbf{x}}\end{aligned} \tag{40}$$

B: Gaussian Random Fields

If we have a variable x drawn from the **probability distribution function** (PDF), $p(x)$, which is normalised to

$$\int_{-\infty}^{\infty} dx\, p(x) = 1 \tag{41}$$

then $p(x)$ is a single-variate **Gaussian random field** (GRF) if x obeys Gaussian statistics and

$$p(x) = \frac{1}{\sqrt{2\pi}\sigma} \exp\left(-\frac{x^2}{2\sigma^2}\right) \tag{42}$$

where σ^2 is the variance. This definition can also be extended to a multi-variate GRF.

The PDF contains the full information of the field. Various useful statistical quantities of the field are **moments** of the field. The first four are:

$$\begin{aligned}
\langle x \rangle &= \int_{-\infty}^{\infty} dx\, x\, p(x) = 0 \\
\left\langle x^2 \right\rangle &= \int_{-\infty}^{\infty} dx\, x^2\, p(x) = \sigma^2 \\
\left\langle x^3 \right\rangle &= \int_{-\infty}^{\infty} dx\, x^3\, p(x) = 0 \\
\left\langle x^4 \right\rangle &= \int_{-\infty}^{\infty} dx\, x^4\, p(x) = 3\sigma^4
\end{aligned} \tag{43}$$

These 4 moments indicate that the field has zero mean (first moment), variance, σ^2, (second moment), zero skewness (third moment), and zero kurtosis (fourth moment). For a single-variate Gaussian random field, all odd moments vanish, and all even moments are given in terms of σ^{2n} [34].

C: Fourier Transforms

The **forward Fourier transform** in n-dimensions is defined as

$$\hat{f}(\omega) = \int_{\mathbb{R}^n} f(x)\, e^{-i\omega \cdot x} dx \tag{44}$$

where ω is the angular frequency. Likewise, the **inverse Fourier transform** in n-dimensions is defined as

$$f(x) = \frac{1}{(2\pi)^n} \int_{\mathbb{R}^n} \hat{f}(\omega)\, e^{i\omega \cdot x} d\omega \tag{45}$$

Fourier transforms are particularly useful for us because of how they transform derivatives. Using integration by parts and the appropriate substitutions, we can convert complicated spatial derivatives in 3D to simple multiplications in Fourier space, as follows [27].

$$\begin{aligned} f(\mathbf{x}) &= \int \frac{d\mathbf{k}}{(2\pi)^3}\, \hat{f}(\mathbf{k})\, e^{-i\mathbf{k}\cdot\mathbf{x}} \\ \nabla f(\mathbf{x}) &= \int \frac{d\mathbf{k}}{(2\pi)^3} - i\mathbf{k}\, \hat{f}(\mathbf{k})\, e^{-i\mathbf{k}\cdot\mathbf{x}} \\ \nabla^2 f(\mathbf{x}) &= \int \frac{d\mathbf{k}}{(2\pi)^3}\, k^2\, \hat{f}(\mathbf{k})\, e^{-i\mathbf{k}\cdot\mathbf{x}} \end{aligned} \tag{46}$$

References

[1] *Dark matter*. URL: https://home.cern/science/physics/dark-matter.

[2] Andrew H. Jaffe. *Cosmology 2012: Lecture Notes*. URL: http://www.sr.bham.ac.uk/~smcgee/ObsCosmo/Jaffe_cosmology.pdf.

[3] E. Corbelli and P. Salucci. "The extended rotation curve and the dark matter halo of M33". In: *Monthly Notices of the Royal Astronomical Society* 311.2 (Jan. 2000), pp. 441–447. ISSN: 1365-2966. DOI: 10.1046/j.1365-8711.2000.03075.x. URL: http://dx.doi.org/10.1046/j.1365-8711.2000.03075.x.

[4] S. M. Faber and R. E. Jackson. "Velocity dispersions and mass-to-light ratios for elliptical galaxies." In: 204 (Mar. 1976), pp. 668–683. DOI: 10.1086/154215.

[5] Steven W. Allen, August E. Evrard, and Adam B. Mantz. "Cosmological Parameters from Observations of Galaxy Clusters". In: 49.1 (Sept. 2011), pp. 409–470. DOI: 10.1146/annurev-astro-081710-102514. arXiv: 1103.4829 [astro-ph.CO].

[6] Alexandre Refregier. "Weak Gravitational Lensing by Large-Scale Structure". In: 41 (Jan. 2003), pp. 645–668. DOI: 10.1146/annurev.astro.41.111302.102207. arXiv: astro-ph/0307212 [astro-ph].

[7] Planck Collaboration et al. "Planck 2015 results. XIII. Cosmological parameters". In: 594, A13 (Sept. 2016), A13. DOI: 10.1051/0004-6361/201525830. arXiv: 1502.01589 [astro-ph.CO].

[8] Douglas Clowe et al. "A Direct Empirical Proof of the Existence of Dark Matter". In: 648.2 (Sept. 2006), pp. L109–L113. DOI: 10.1086/508162. arXiv: astro-ph/0608407 [astro-ph].

[9] E. Komatsu et al. "Five-Year Wilkinson Microwave Anisotropy Probe Observations: Cosmological Interpretation". In: 180.2 (Feb. 2009), pp. 330–376. DOI: 10.1088/0067-0049/180/2/330. arXiv: 0803.0547 [astro-ph].

[10] Tom Metcalfe. *Maybe 'dark matter' doesn't exist after all, new research suggests*. Jan. 2021. URL: https://www.nbcnews.com/science/space/maybe-dark-matter-doesn-t-exist-after-all-new-research-n1252995.

[11] Martín López-Corredoira. "Problems with the dark matter and dark energy hypotheses, and alternative ideas". In: *The multi-messenger astronomy: gamma-ray bursts, search for electromagnetic counterparts to neutrino events and gravitational waves. Proceedings of the International Conference.* (2019). DOI: 10.26119/sao.2019.1.35528. URL: http://dx.doi.org/10.26119/SAO.2019.1.35528.

[12] M. Milgrom. "A modification of the Newtonian dynamics as a possible alternative to the hidden mass hypothesis." In: 270 (July 1983), pp. 365–370. DOI: 10.1086/161130.

[13] Pavel Kroupa, Marcel Pawlowski, and Mordehai Milgrom. "The Failures of the Standard Model of Cosmology Require a New Paradigm". In: *International Journal of Modern Physics D* 21.14, 1230003 (Dec. 2012), p. 1230003. DOI: 10.1142/S0218271812300030. arXiv: 1301.3907 [astro-ph.CO].

[14] Ella Alderson. *Doubting Dark Matter*. July 2019. URL: https://medium.com/predict/doubting-dark-matter-f3e400c7dcd7.

[15] Luca Di Luzio et al. "The landscape of QCD axion models". In: 870 (July 2020), pp. 1–117. DOI: 10.1016/j.physrep.2020.06.002. arXiv: 2003.01100 [hep-ph].

[16] Marco Drewes. "The Phenomenology of Right Handed Neutrinos". In: *International Journal of Modern Physics E* 22.8, 1330019-593 (Aug. 2013), pp. 1330019–593. DOI: 10.1142/S0218301313300191. arXiv: 1303.6912 [hep-ph].

[17] M. Kamionkowski. "WIMP and Axion Dark Matter". In: *High Energy Physics and Cosmology, 1997 Summer School*. Ed. by E. Gava et al. Vol. 14. Jan. 1998, p. 394. arXiv: hep-ph/9710467 [hep-ph].

[18] J. M. Overduin and P. S. Wesson. "Dark matter and background light". In: 402.5-6 (Nov. 2004), pp. 267–406. DOI: 10.1016/j.physrep.2004.07.006. arXiv: astro-ph/0407207 [astro-ph].

[19] Matt Williams. *Dark matter-hot or not?* Aug. 2016. URL: https://phys.org/news/2016-08-dark-matterhot.html.

[20] *Astronomy 123: Galaxies and the Expanding Universe*. URL: http://abyss.uoregon.edu/~js/ast123/lectures/lec24.html.

[21] Gianfranco Bertone, Dan Hooper, and Joseph Silk. "Particle dark matter: evidence, candidates and constraints". In: 405.5-6 (Jan. 2005), pp. 279–390. DOI: 10.1016/j.physrep.2004.08.031. arXiv: hep-ph/0404175 [hep-ph].

[22] Nick Strobel. *Universe is Uniform on Large Scales*. Dec. 2020. URL: http://www.astronomynotes.com/cosmolgy/s3.htm.

[23] Daniel Baumann. "Cosmology: Part III Mathematical Tripos". URL: https://www.damtp.cam.ac.uk/user/examples/3R2La.pdf.

[24] Furqaan Yusaf. "Dark Matter and Dark Energy".

[25] Malcolm Fairbairn. "Dark Matter and Dark Energy".

[26] David H. Weinberg. "A873: Cosmology VIII. Linear Fluctuations". URL: http://www.astronomy.ohio-state.edu/~dhw/A873/notes8.pdf.

[27] Ried van de Weygaert. "Large Scale Structure (2009)". URL: https://www.astro.rug.nl/~weygaert/tim1publication/lss2009/lss2009.linperturb.pdf.

[28] P. J. E. Peebles. *The large-scale structure of the universe*. Provided by the SAO/NASA Astrophysics Data System. 1980. URL: https://ui.adsabs.harvard.edu/abs/1980lssu.book.....P.

[29] Scott Dodelson and Fabian Schmidt. *Modern Cosmology*. Academic Press, an imprint of Elsevier, 2003. URL: https://pdfcoffee.com/modern-cosmology-scott-dodelson-2nd-edition-4-pdf-free.html.

[30] Marc Kamionkowski. "AY127: Cosmology. The growth of density perturbations". URL: https://sites.astro.caltech.edu/~george/ay127/kamionkowski-perturbations-notes.pdf.

[31] Miguel Zumalacárregui. "The Cosmic Linear Anisotropy Solving System: a most classy way from Fundamental Physics to Cosmology". URL: http://miguelzuma.github.io/hi_class/hi_class_course_IFT.pdf.

[32] N. Aghanim et al. "Planck 2018 results". In: *Astronomy Astrophysics* 641 (Sept. 2020), A6. ISSN: 1432-0746. DOI: 10.1051/0004-6361/201833910. URL: http://dx.doi.org/10.1051/0004-6361/201833910.

[33] Gianpiero Mangano et al. "Relic neutrino decoupling including flavour oscillations". In: *Nuclear Physics B* 729.1 (2005), pp. 221–234. ISSN: 0550-3213. DOI: https://doi.org/10.1016/j.nuclphysb.2005.09.041. URL: https://www.sciencedirect.com/science/article/pii/S0550321305008291.

[34] Marjolein Dijkstra. *AST4320: LECTURE 6*. URL: https://www.uio.no/studier/emner/matnat/astro/AST4320/h14/timeplan/lecture6note%281%29.pdf.